Lasers in Surgery and Medicine 29:128–135 (2001)

Fluorescence Spectroscopy for In Vivo Characterization of Ovarian Tissue

Molly Brewer, DVM, MD, MS,[1,2] Urs Utzinger, PhD,[3] Elvio Silva, MD,[4] David Gershenson, MD,[2] Robert C. Bast, Jr., MD,[5] Michele Follen, MD, PhD,[1,2] and Rebecca Richards-Kortum, PhD[3]*

[1]*Department of Gynecology, The University of Texas Medical School, Houston, Texas 77030*
[2]*Department of Gynecologic Oncology, The University of Texas, M.D. Anderson Cancer Center, Houston, Texas 77030*
[3]*Biomedical Engineering Program, The University of Texas at Austin, Austin, Texas 78712*
[4]*Department of Pathology, The University of Texas, M.D. Anderson Cancer Center, Houston, Texas 77030*
[5]*Division of Translational Research, The University of Texas, M.D. Anderson Cancer Center, Houston, Texas 77030*

Background and Objective: The objective of this study was to explore whether fluorescence spectroscopy signatures differed between normal variations within the ovary, benign neoplasms, and ovarian cancer.

Study Design/Materials and Methods: Ovarian tissue fluorescence emission spectra were collected sequentially at 18 excitation wavelengths ranging from 330 to 500 nm from 11 patients undergoing oophorectomy and assembled into fluorescence excitation emission matrices (EEMs); biopsies corresponded to the area interrogated. Spectral areas that could differentiate normal ovary, benign neoplasms, and cancers were evaluated, using histopathology as the reference standard.

Results: The most promising measurements are (1) the integrated fluorescence intensity from 400 to 430 nm excitation at 460 nm emission, and (2) the ratios of fluorescence intensities at 330 nm excitation, 385 and 500 nm emission, and at 375 and 415 nm excitation, 460 nm emission. Simple systems to visualize these optical signatures at laparoscopy could be designed.

Conclusion: Fluorescence spectroscopy may have the ability to distinguish ovarian cancers from normal ovarian structures and benign neoplasms, as well as differentiate between normal variations and metaplastic structures and should be further explored as a device for the early detection of ovarian cancers. Lasers Surg. Med. 29:128–135, 2001.

Key words: fluorescence spectroscopy; ovarian cancer detection

INTRODUCTION

Ovarian cancer causes the highest mortality of any of the gynecologic cancers and is the second most common gynecologic malignancy [1]. Women with Federation of International Gynecology and Obstetrics (FIGO) Stage I disease have a 5-year survival of 80–90% [2], while women with FIGO Stage III or IV disease have a 5-year survival of 5–30%. Unfortunately, 70% of all ovarian cancers are diagnosed in Stage III or IV. Patients would have a significantly improved survival if their cancer could be detected while still limited to the ovary [3]. There is widespread interest in developing screening methods for early ovarian cancer because of the high mortality associated with the Stages II–IV. There is no single screening test for ovarian cancer that has adequate efficacy [4]. The available screening tests, CA125 [5,6], trans-vaginal ultrasound [7,8], and pelvic exam, lack evidence of acceptable sensitivity, and specificity [4].

Mutations in the BRCA1 and BRCA2 genes or a strong family history of breast and/or ovarian cancer have been strongly linked to an increased susceptibility to both breast and ovarian cancer. The lifetime risk of ovarian cancer for women with BRCA1 mutation may be as high as 40% while the risk for women with BRCA2 mutations may be as high as 10% [9]. Using family history and genetic testing, we can identify those women at higher than average risk for developing ovarian cancer. This group of women needs effective methods to detect ovarian cancer at a preinvasive or early stage and is the group of women targeted for this technology.

Techniques based on quantitative optical spectroscopy have shown promise to improve detection of epithelial lesions in the colon, cervix, bladder, head and neck, esophagus, and other epithelial surfaces [10–12]. A number of optical spectroscopy techniques have been examined for detection of epithelial neoplasms, including diffuse reflectance spectroscopy, fluorescence spectroscopy, and Raman spectroscopy. Algorithms can be developed to analyze tissue fluorescence and identify early neoplastic changes as they occur in situ. The goal of the work presented in this paper is to explore whether fluorescence spectroscopy could eventually be adapted to improve early diagnosis of ovarian neoplasia.

METHODS

Patients

The study was reviewed and approved by the Institutional Review Boards of The University of Texas at Austin

*Correspondence to: Dr. Rebecca Richards-Kortum, Department of Electrical and Computer Engineering, The University of Texas at Austin, Austin, TX 78712.
E-mail: kortum@mail.utexas.edu
Accepted 12 March 2001

and M.D. Anderson Cancer Center, Hermann Hospital, and Lyndon Baines Johnson Hospital. Patients undergoing exploratory laparotomy and oophorectomy at The University of Texas M.D. Anderson Cancer Center, Hermann Hospital, and Lyndon B. Johnson (LBJ) Harris County Hospital in Houston, Texas, were asked to participate in this in vivo fluorescence spectroscopy study. Informed consent was obtained from each patient who participated. At the time of exploratory laparotomy, fluorescence spectra were acquired from two to six sites, both normal and abnormal in appearance, prior to disrupting the blood supply. Tissue biopsies were obtained from all sites after they had been identified visually and analyzed by the probe.

Pathology

At the time of laparotomy, all specimens were collected from the area that was interrogated optically and fixed in formalin. Hematoxylin and eosin staining was done in the standard manner and slides were examined by a single gynecologic pathologist (ES) who was blinded to the spectroscopy results. Samples were classified into eight categories based on the most prevalent pathology, which included normal ovary, stromal hyperplasia, corpus luteum, corpus albicans, endosalpingiosis, inclusion cyst, benign neoplasm, or cancer. Cancers ranged from Stages I to III (Federation of International Gynecology and Obstetrics (FIGO) Staging) and were all high grade carcinoma. For purposes of classification, samples were grouped into four categories: normal, endosalpingiosis, benign neoplasm, and cancer.

Data Acquisition

The spectroscopic system is briefly summarized here but is described in more detail elsewhere [13]. Figure 1a shows a schematic block diagram of the system, which can be easily utilized in the average operating suite. It consists of a Xenon arc lamp coupled to a scanning monochromator to provide a tunable source of monochromatic excitation. A fiber optic probe (Fig. 1b) which directs excitation light to the tissue, collects emitted fluorescence light, and delivers it to an imaging spectrograph and CCD camera. The probe collects fluorescence over a 2 mm circular diameter. A short piece of a thick optical fiber acts as a shield, and both excitation and collected light passes through this shield. Fluorescence emission spectra are collected sequentially at 18 excitation wavelengths ranging from 330 to 500 nm in 10 nm increments and assembled into a fluorescence excitation emission matrix (EEM). The time required to collect all fluorescence measurements is 2.5 min.

Data Analysis

All spectra were reviewed by a single investigator blinded to the pathologic results (UU). Spectra were discarded if their computer files were not saved properly due to software error or if fluorescence values were very low or negative, indicating that the probe was not in proper contact with the tissue or that the background was not measured accurately.

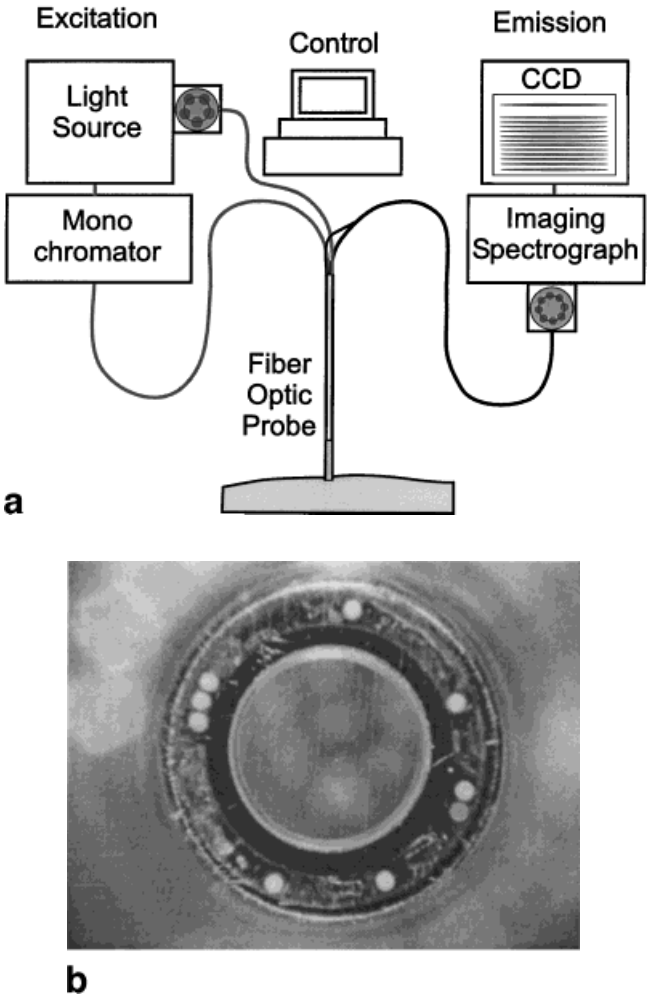

Fig. 1. **a**: Schematic diagram of system used to measure fluorescence excitation emission matrices. **b**: Picture of fiber optic probe tip. The fluorescence collection channel is the inner glass tube that is embedded into a metallic tubing. Reflected white light can be measured with fibers placed along the circumference of the probe.

All EEMs were examined visually by three investigators (UU, RRK, MB) to identify those excitation and emission wavelengths where consistent changes were observed between samples in the eight diagnostic categories. For further data analysis, samples were grouped into the four categories felt to be the most diagnostically important: normal ovary, endosalpingiosis, benign neoplasm, and cancer. From the visual inspection of all EEMs, we identified those excitation and emission wavelengths that visually showed the most promising differences between the four categories. At each selected excitation wavelength, mean emission spectra were calculated for each of the four categories, and all spectra and means were plotted. Similarly, at each emission wavelength, mean excitation spectra were calculated and all spectra were plotted. Spectra were then examined visually to identify those wavelength

TABLE 1. Summary of Data Pathology and Sites Measured

Patient	Normal	Cyst	Corpus Luteum	Corpus Albicans	Hyperplasia	Endo-salpingiosis	Benign Neoplasm	Cancer	Age
1	1			1	1	1			62
2				1	3				69
3*	2	1				3			31
4					1		3		49
5	2			1			1		52
6								2	49
7				2	4				75
8						4			50
9					1		3		44
10*	4	1	2						34
11				2				1	54

*denotes premenopausal patients.

combinations where there were the largest and most consistent changes between the four categories. All calculations and graphs were produced using Matlab® (Mathworks, Inc. Natick, MA) and the Statistics Toolbox for Matlab.

RESULTS

Twenty patients were enrolled in the study and the probe was placed on the tissue in 76 total sites. Data was excluded or not available for analysis because of device or software failure, missing pathology or exclusion by blinded visual review. There were 48 evaluable measurements from 11 patients. The diagnostic categories are outlined in Table 1, and include 30 measurements of normal ovaries, eight of endosalpingiosis, seven of benign neoplasms (adenofibroma), and three measurements of carcinoma.

Figure 2 shows EEMs of normal ovary and ovarian cancer from a representative patient in the study. Figure 2a shows an EEM from a site of normal ovarian stroma and a corpus albicans; Figure 2b shows a photomicrograph of the pathology of the area interrogated. Figure 2c shows an EEM from an ovarian site with high-grade carcinoma and adjacent stroma which is normal; Figure 2d shows a photomicrograph of the area interrogated. Fluorescence peaks were found in both graphs at 330 nm excitation, 380 nm emission (consistent with structural protein cross-link fluorescence), 350 nm excitation and 460 nm emission (consistent with NADH fluorescence), and 450 nm excitation, 520 nm emission (consistent with FAD fluorescence). In addition, valleys are present at 420 nm excitation and emission, consistent with absorption of hemoglobin. The effects of hemoglobin absorption are much greater in the EEM corresponding to the high-grade carcinoma. We examined excitation and emission spectra corresponding to regions where differences in the fluorescence of neoplastic and non-neoplastic ovary were most consistently noted. In particular, emission spectra at 330 nm excitation and excitation spectra at 460 nm emission showed consistent differences.

The top row of Figure 3 shows emission spectra of all samples by diagnostic category at 330 nm excitation. The bottom row of Figure 3 shows excitation spectra at 460 nm emission for all samples by diagnostic category. In addition, average spectra are shown for each of the four diagnostic categories. At 330 nm excitation, the cancers show increased fluorescence at 380 nm emission and decreased fluorescence above 450 nm emission. At 460 nm emission, the cancers show increased fluorescence at 330–360 nm excitation and decreased fluorescence at 400–430 nm excitation. The decrease in fluorescence at 400–430 nm excitation and 460 nm emission was consistently observed in all cancers measured. Figure 4 shows a box and whisker plot indicating the integrated intensity over this range for all samples measured by diagnostic category. The box has lines at the lower quartile, median, and upper quartile values. The whiskers are lines extending from each end of the box to show the extent of the rest of the data. Outliers are data with values beyond the ends of the whiskers. The mean integrated intensity was lowest in the cancers. While the variance is large and the numbers are small, the mean integrated intensity of the cancers was statistically significantly different than the normal ($P < 0.01$) and benign ($P < 0.02$) categories. Further, a simple diagnostic algorithm, which classifies samples as cancer if the integrated fluorescence intensity in this region is less than 0.08, correctly classifies all cancer samples and all but one of the normal and benign samples.

Figure 5 presents a second simple diagnostic algorithm based on changes in fluorescence at 330 nm excitation and 460 nm emission. This scatterplot shows the ratio of fluorescence intensities at 330 nm excitation, 385 and 500 nm emission plotted on the ordinate vs. the ratio of fluorescence intensities at 375 and 415 nm excitation, 460 nm emission plotted on the abscissa. A linear decision

line separates all samples with cancer from benign tumors and other normal ovarian structures.

DISCUSSION

While this is an exploratory study, results indicate that simple algorithms based on autofluorescence have the potential to identify the presence of ovarian cancer in vivo. This is potentially important, because ovarian cancer is usually diagnosed in Stage III or IV, and has less than a 30% 5-year survival. New technologies that could provide earlier detection could have an enormous clinical impact.

An important advantage of the simple algorithms proposed here is that it can be implemented with a simple system through the laparascope. For example, coupling the laparascope to an illumination source from 400 to 430 nm excitation, and filtering the detected light at 460 nm emission would enable a physician to examine the ovarian surface and search for areas of decreased

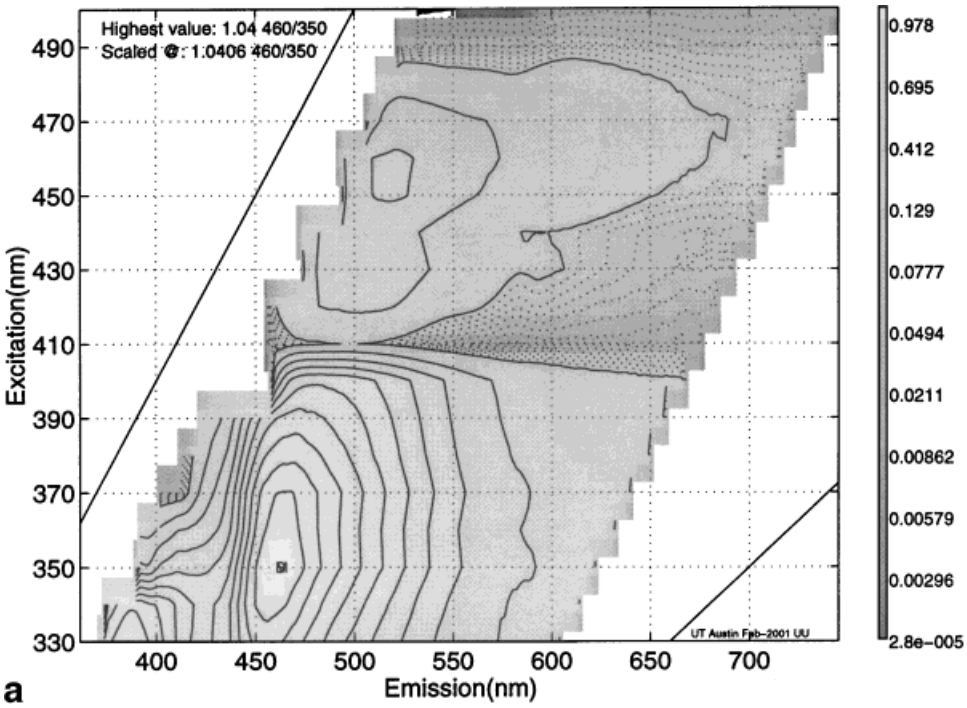

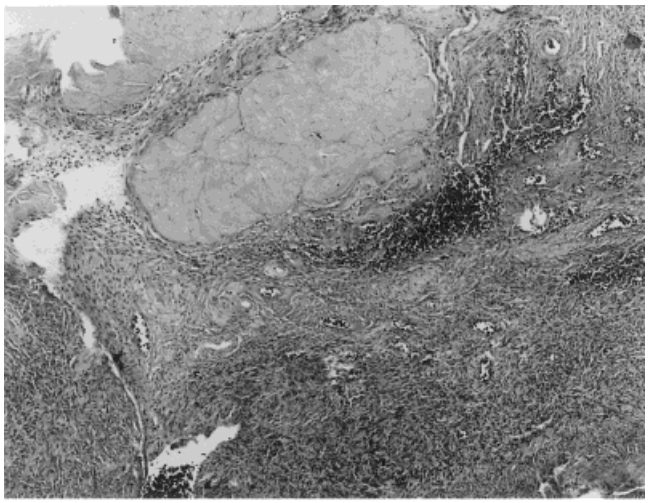

Fig. 2. (**a**). EEM of normal ovary with stromal hyperplasia and corpus albicans. (**b**). Pathology corresponding to EEM in Figure 2(a). (**c**). EEM of ovarian high grade carcinoma. (**d**). Pathology corresponding to EEM in Figure 2(c).

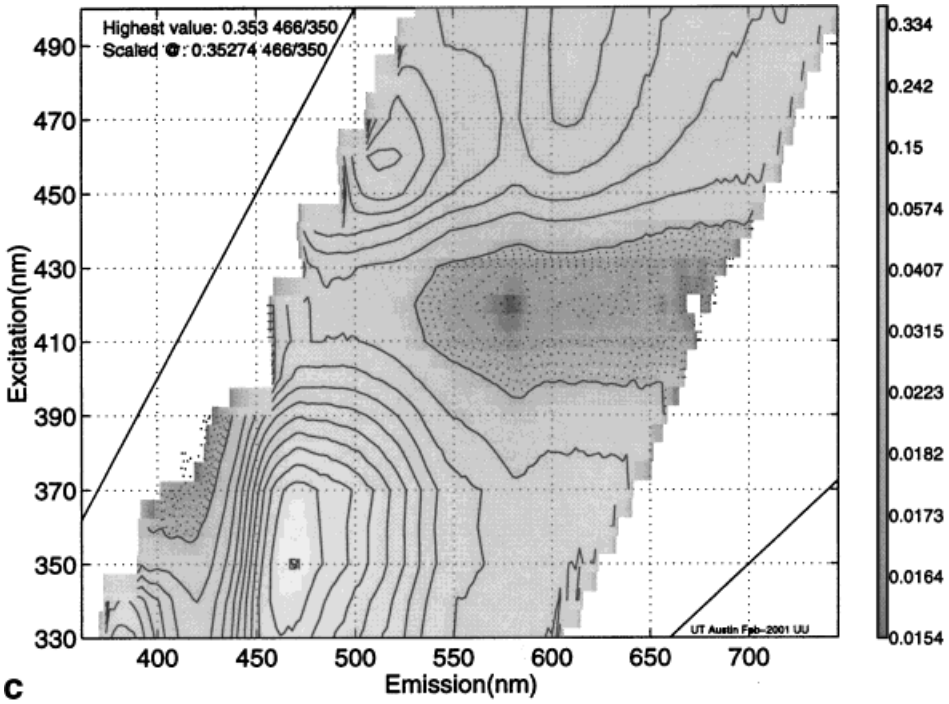

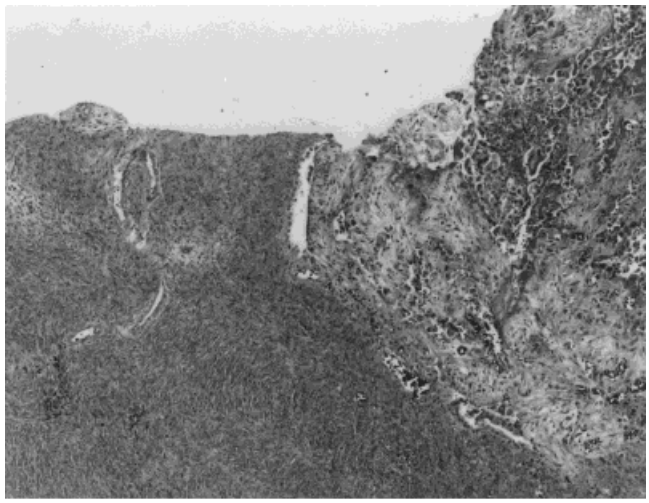

Fig. 2. (*Continued*)

fluorescence. Figure 6 illustrates the type of image that would result. Figure 6a shows an ovary photographed under white light while Figure 6b and c shows autofluorescence of an ovary in vitro at 400 to 350 nm excitation. The ovary was removed at the time of surgery and immediately placed under monochromatic excitation light. The fluorescence was easily visible by eye, and was documented through a long pass filter using a 35 mm camera. The areas showing strongest fluorescence seems to originate from collagen structures. Blood vessels show a good contrast to the surrounding area with decreased intensity. Some yellow fluorescence spots can be observed while other areas show a green fluorescence.

In this pilot study, fluorescence excitation at 330, 375, and 415 nm appear useful diagnostically. Differences found at these wavelengths are likely due to a combination of changes in both autofluorescence and reabsorption of autofluorescence. In particular, decreased fluorescence at 415 nm excitation by neoplastic samples is likely due to increased absorption of the excitation light by hemoglobin

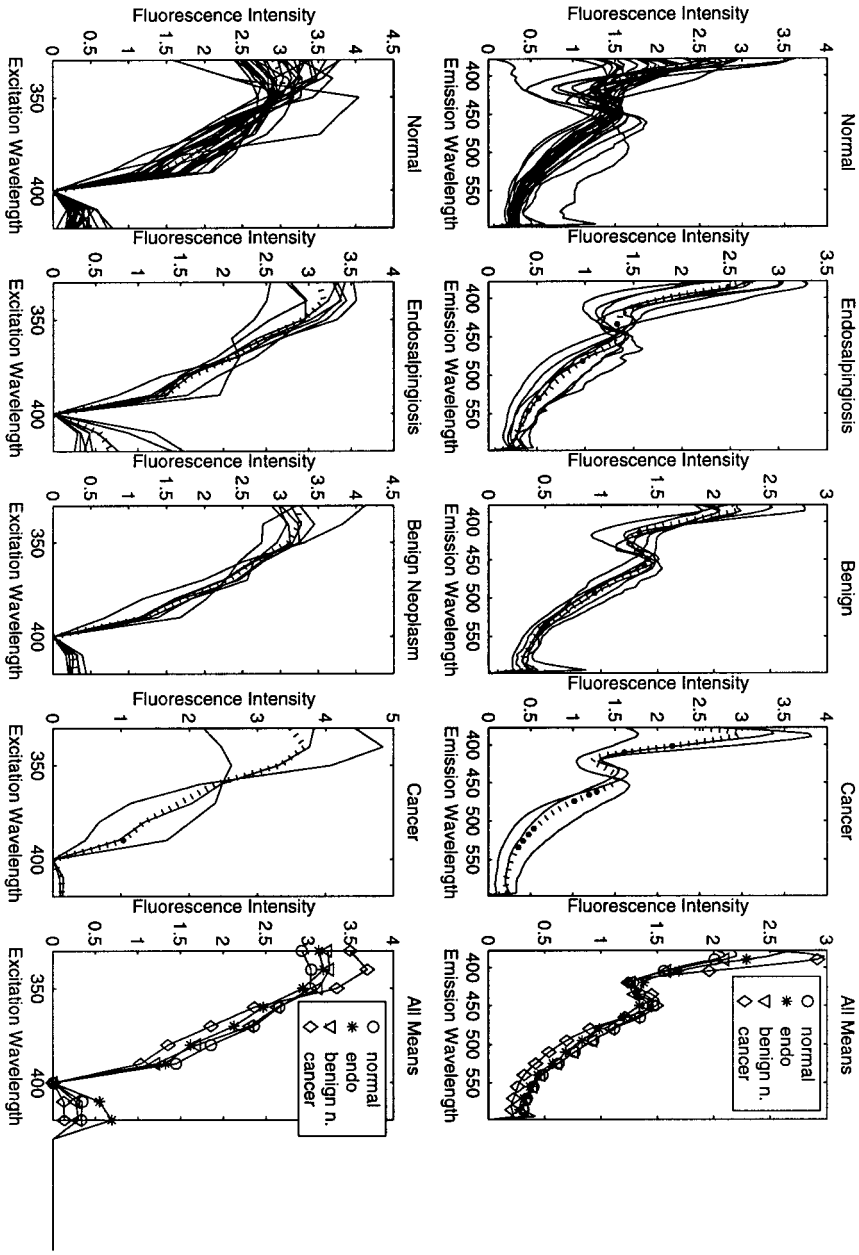

Fig. 3. Top Row: Fluorescence emission spectra at 330 nm excitation by diagnostic category. Bottom Row: Fluorescence excitation spectra at 460 nm emission by diagnostic category.

which could be attributed to angiogenesis. This is consistent with the increased ratio of fluorescence at 375 nm excitation, 460 nm emission to that at 415 nm excitation, and 460 nm emission. Differences at 330 nm excitation can be attributed to changes in the fluorescence of structural proteins, NADH, and reabsorption due to hemoglobin. The source of these changes can be explored using fluorescence microscopy of short-term tissue cultures [14]. This pilot study suggests that such microscopy of normal and neoplastic ovarian tissue should be carried out at 330, 375, and 415 nm excitation.

Although the numbers of cancers were low in this series, the great variability of the structural changes measured and evaluated in the ovarian surface and subsurface provides valuable information for developing spectroscopy both to screen for ovarian cancer and to potentially evaluate women for occult neoplasms. Fluorescence spectroscopy has been shown to be more sensitive and specific

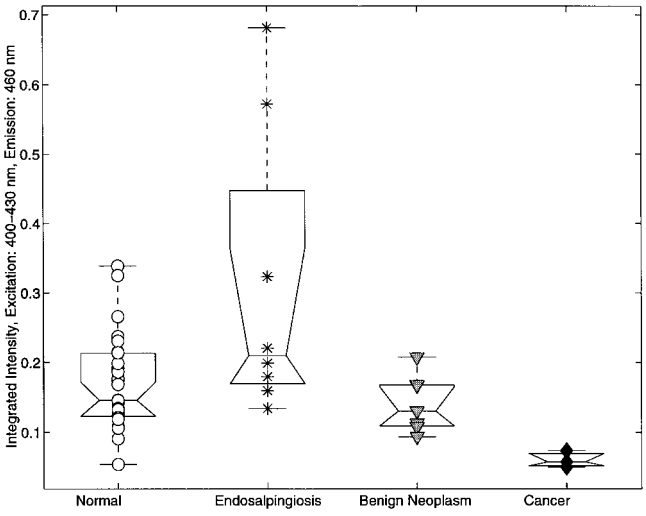

Fig. 4. Box and whiskers plot showing integrated fluorescence intensity from 400–430 nm excitation at 460 nm emission.

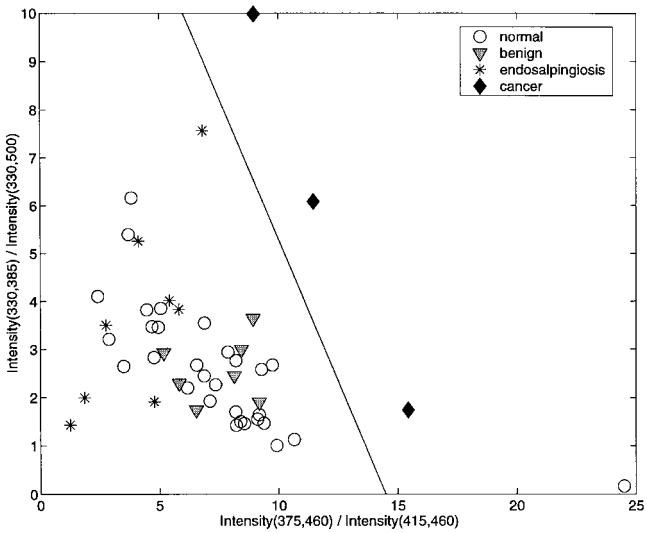

Fig. 5. Scatterplot showing ratio of fluorescence intensities at 330 nm excitation, 385 and 500 nm emission. A simple linear diagnostic algorithm correctly separates all cancers from benign neoplasms and normal ovarian structures.

than traditional methods of surface microscopy in other organ systems, such as the cervix, to identify early preneoplastic changes and thus shows promise in the ovary. This could be particularly useful in BRCA-positive women who may have a higher rate of occult neoplasms in the ovary. Fluorescence imaging and spectroscopy may provide a new tool to detect subtle differences not appreciable either with ultrasound or visual observation of the ovary. Further study of this methodology with larger number of cancers and patients with normal ovaries is warranted, given the results of this pilot study.

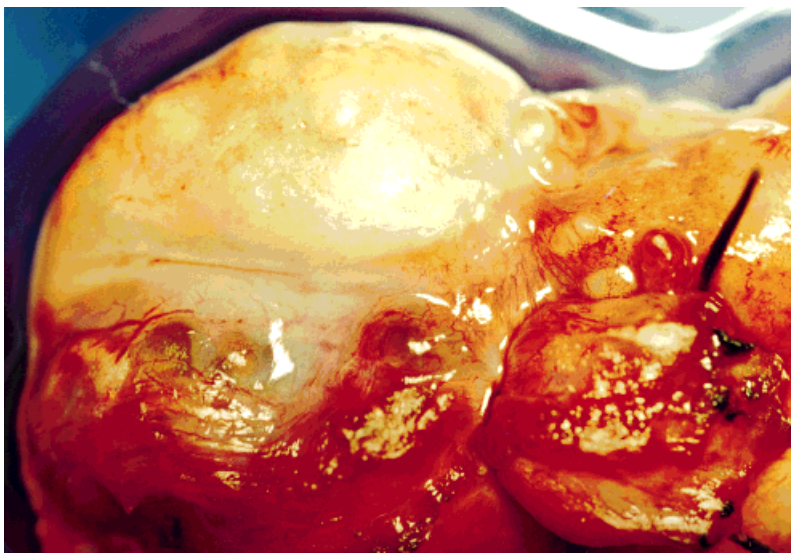

Fig. 6. Normal ovary under white light (**a**) and autofluorescence of ovary photographed at 400 nm excitation (**b**) and 350 nm (**c**) excitation.

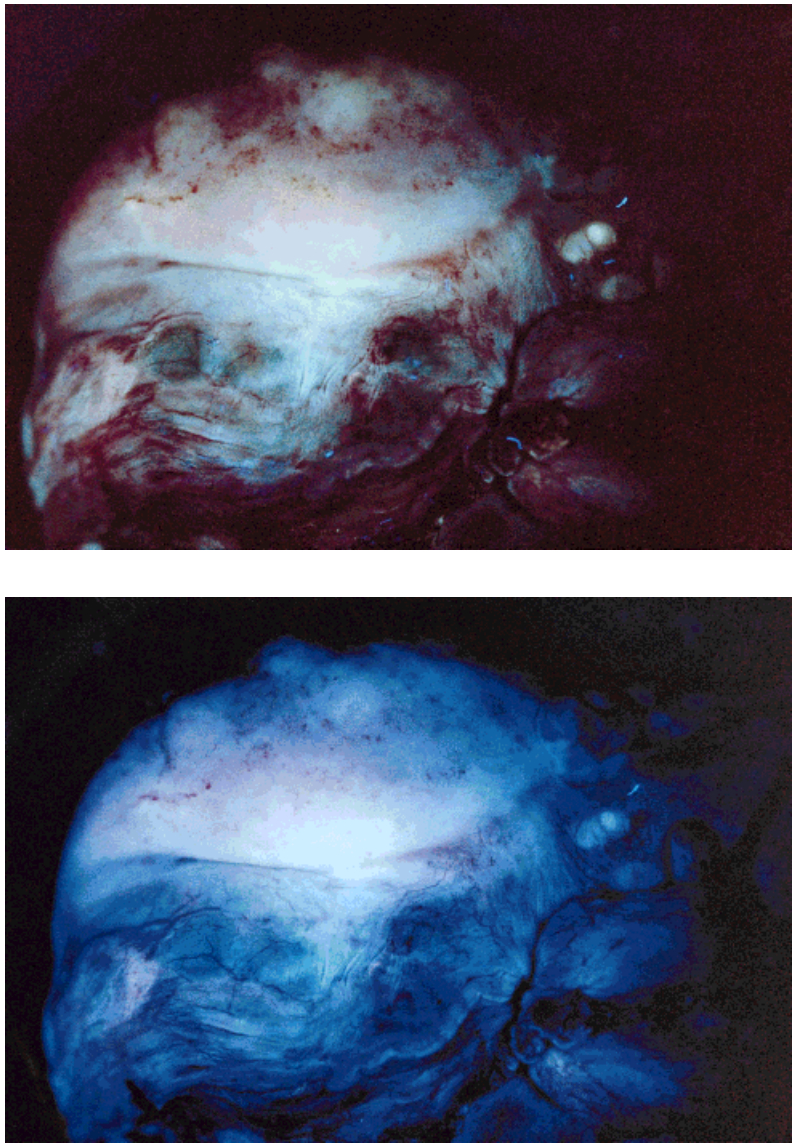

Fig. 6. (*Continued*)

REFERENCES

1. American Cancer Society. www.cancer.org.
2. Wingo PA, Tong T, Bolden S. Cancer statistics. Ca Cancer J Clin 1995;45(1):8–30.
3. Hoskins WJ. Prospective on ovarian cancer: Why prevent? J Cell Biochem Suppl 1995;23:189–199.
4. NIH Consensus Development Panel on Ovarian Cancer. Ovarian cancer screening, treatment and follow-up. JAMA 1995;273:491–497.
5. de Bruijn HW, van der Zee AG, Aalders JG. The value of cancer antigen 125 (CA 125) during treatment and follow-up of patients with ovarian cancer. Curr Opin Obstet Gynecol 1997;9(1):8–13.
6. Berek JS, Bast Jr, RC. Ovarian cancer screening. The use of serial complementary tumor markers to improve sensitivity and specificity for early detection. Cancer 1995;76(10):2092–2096.
7. Karlan BY: The status of ultrasound and color Doppler imaging for the early detection of ovarian carcinoma. Cancer Invest 1997;15(3):265–269.
8. Van Nagell Jr, JR, DePriest PD, Puls LE, et al. Ovarian cancer screening in asymptomatic postmenopausal women by transvaginal sonography. 1991; Cancer 68(3):458–462.
9. Burke W, Daly M, Garber J, et al. Recommendations for follow-up care of individuals with an inherited predisposition to cancer. JAMA 1997;277(12):997–1003.
10. Wagnieres GA, Star WM, Wilson BC. In vivo fluorescence spectroscopy and imaging for oncological applications. Photochem Photobiol 1998;68(5):603–632.
11. Mahadevan-Jansen A, Richards-Kortum R. Raman spectroscopy for the detection of cancers and precancers. J Biomed Opt 1996;1(1):31–70.
12. Bigio IJ, Mourant JR. Ultraviolet and visible spectroscopies for tissue diagnostics: fluorescence spectroscopy and elastic-scattering spectroscopy. Phys Med Biol 1997;42(5):803–814.
13. Zuluaga AF, Utzinger U, Durkin A, et al. Fluorescence excitation emission matrices of human tissue: a system for in vivo measurement and method of data analysis. Appl Spectrosc 1998;53(3)301:11.
14. Brookner CK, Follen M, Boiko I, et al. Autofluorescence patterns in short-term cultures of normal cervical tissue. Photochem Photobiol 2000;71(6):730–736.